

ON THE COMPUTATION OF THE SLOW DYNAMICS OF NONLINEAR MODES OF MECHANICAL SYSTEMS

Malte Krack^{1,*}, Lars Panning-von Scheidt¹, Jörg Wallaschek¹

Abstract

A novel method for the numerical prediction of the slowly varying dynamics of nonlinear mechanical systems has been developed. The method is restricted to the regime of an isolated nonlinear mode and consists of a two-step procedure: In the first step, a multiharmonic analysis of the autonomous system is performed to directly compute the amplitude-dependent characteristics of the considered nonlinear mode. In the second step, these modal properties are used to construct a two-dimensional reduced order model (ROM) that facilitates the efficient computation of steady-state and unsteady dynamics provided that nonlinear modal interactions are absent.

The proposed methodology is applied to several nonlinear mechanical systems ranging from single degree-of-freedom to Finite Element models. Unsteady vibration phenomena such as approaching behavior towards an equilibrium point or limit cycles, and resonance passages are studied regarding the effect of various nonlinearities such as cubic springs, unilateral contact and friction. It is found that the proposed ROM facilitates very fast and accurate analysis of the slow dynamics of nonlinear systems. Moreover the ROM concept offers a huge parameter space including additional linear damping, stiffness and near-resonant forcing.

Keywords: nonlinear modes, invariant manifolds, nonlinear modal analysis,

*Corresponding author

Email address: krack@ila.uni-stuttgart.de (Malte Krack)

nonlinear modal synthesis, slow dynamics, reduced order modeling, averaging

Nomenclature

a	Modal amplitude
\mathbf{f}	Nonlinear force vector
i	Imaginary unit
$\mathbf{M}, \mathbf{C}, \mathbf{K}$	Mass, damping, stiffness matrices
N_h	Harmonic order of Fourier ansatz
t	Time
\mathbf{u}	Displacement vector
\mathbf{u}_p	Periodic form of displacement vector
\mathbf{v}	Complex eigenvector
λ, ω_0, D	Eigenvalue, eigenfrequency, damping ratio
Ω	Angular frequency of oscillation
φ, φ_e	Fast phase, fast phase induced by excitation
Ψ_n	N-th harmonic of eigenvector
Θ	Slow phase
ϑ	Absolute phase
$(\dot{}), (\ddot{})$	First and second-order derivative with respect to time t
$(\bar{})$	Complex conjugate
$()^T$	Transpose
$()^H$	Hermitian transpose
$\langle \cdot, \cdot \rangle$	Inner product
DOF	Degree of freedom
FE	Finite Element
HBM	(High-order) Harmonic Balance Method
NMA	Nonlinear Modal Analysis
ODE	Ordinary Differential Equation
ROM	Reduced Order Model

1. Introduction

1.1. *Motivation for reduced order modeling of nonlinear systems*

In many structural dynamic systems, the effect of nonlinearity plays an important role. In fact, several engineering applications exploit nonlinear phenomena in order to improve the dynamic behavior of mechanical structures. Hence, there is a considerable need for efficient and versatile methods for the dynamic analysis of such systems.

For systems that comprise a large number of degrees of freedom (DOFs) and exhibit generic nonlinearities, as addressed in this study, the applicability of analytical methods is typically not possible and numerical methods have to be employed. The application of direct solution methods such as time-step integration often results in high computational costs. Therefore, extensive parametric studies, sensitivity and uncertainty analyses or design optimization soon become infeasible in conjunction with the full order model. Thus, there is a demand for Reduced Order Models (ROM) that are capable of significantly reducing the computational effort for the dynamic analysis and retaining the required accuracy of the predicted results.

1.2. *Existing approaches*

Methods based on the invariant manifold approach [1, 2, 3, 4, 5] are widely-used for the modal analysis of nonlinear mechanical systems as well as for the construction of efficient ROMs. The approach is based on the invariance property of certain periodic orbits of the dynamical systems, i. e. a nonlinear mode is defined as an invariant relationship (manifold) between several master coordinates and the remaining coordinates of the system. This manifold is typically governed by partial differential equations arising from the substitution of the manifold into the state form of the equations of motion. The invariant manifold approach was extended to account for the effect of harmonic excitation [3] and viscous damping [5]. It has been applied to various problems including piecewise linear systems [6], internally resonant nonlinear modes [4] and generic

nonlinearly damped systems [7].

A straight-forward ROM strategy consists of constraining the system dynamics to the computed invariant manifold. This strategy is capable of drastically reducing the dimensionality of the problem to only a few master coordinates, while providing excellent accuracy for steady-state as well as unsteady dynamic predictions. One drawback is, however, the huge effort for the computation of the invariant manifolds. These computations can involve several thousands of nonlinearly coupled algebraic equations [3]. Moreover, the development of numerically robust algorithms for the treatment of generic, in particular non-conservative nonlinearities, seems to be an unresolved problem, see e. g. [7]. Furthermore, since the time-dependency is lost in the problem definition, the characteristic frequencies cannot directly be obtained from the computed manifold, but has to be identified from simulation results [6, 7]. Finally, the parameter space of the ROM based on the invariant manifold approach is typically limited. For example, harmonic excitation and viscous damping are generally considered in the manifold computation step [3, 5] so that even slight modification of these parameters would require the re-computation of the manifold.

Another category of methods for the determination of modal properties of nonlinear systems can be classified as nonlinear system identification (NSI) approaches [8, 9, 10, 11]. Response data, obtained either by simulation or measurement, is gathered and modal properties are identified by fitting original response data to data from nonlinear modal synthesis. The weak point of this strategy is clearly its signal-dependent nature and the further effort required to obtain the response data. One of the main benefits of this method is that no model is required for the nonlinearities which enables broad applicability. Modal properties identified with NSI methods can be easily employed to feed the parameters of a nonlinear ROM [8, 9].

Harmonic Balance approaches are widely used for the nonlinear modal analysis of conservative mechanical systems [12, 13, 14]. These methods are generally

known to be well-suited for the analysis of strongly nonlinear systems with a large number of DOFs. Recently, LAXALDE AND THOUVEREZ [15] extended the Harmonic Balance Method to the approximate modal analysis of dissipative systems by introducing a complex eigenfrequency in the Fourier ansatz. KRACK ET AL. [16, 17] applied this approach to various nonlinear mechanical systems and significantly improved the numerical performance of the analysis. This frequency-domain modal analysis concept allows for the direct calculation of iso-energy orbits on the invariant manifold as well as eigenfrequency and modal damping ratio of the nonlinear system. The modal properties have also been exploited in a ROM formulation for the prediction of steady-state vibrations [15, 16, 17]. KRACK ET AL. [16, 17] also investigated the limitations of the ROM and demonstrated that the validity of this approach is restricted to those regimes in which the energy is confined to a single nonlinear mode. This finding is completely in line with the work of BLANC ET AL. [18], who concluded that the absence of nonlinear modal interactions represents an intrinsic limitation to ROMs based on the invariant manifold concept.

1.3. Need for research regarding approaches for unsteady dynamics

For various engineering applications, it is important to assess the transient dynamics induced ‘on the way to’ the operating point, if it exists. Most of the above mentioned ROM concepts are, however, designed to predict the steady-state vibration behavior of nonlinear systems. Among the few existing approximation methods for the slow dynamics of nonlinear systems, complexification-averaging is probably the most commonly used technique [19, 20, 21, 22]. This technique is, however, typically applied to obtain closed-form analytical solutions for systems featuring polynomial nonlinearities and only a small number of degrees of freedom.

In order to obtain a concept for generic nonlinear systems, this study builds on the broadly applicable multi-harmonic nonlinear modal analysis technique developed in [15, 16]. The original problem and considered dynamic regime is described in section 2. The generalized Fourier-Galerkin method is briefly re-

visited in section 3. For the first time, the averaging technique is applied to the thus defined nonlinear modes in section 4 to obtain approximations for the slow dynamics on the invariant manifold of an isolated nonlinear mode. In order to assess the performance and validity of the proposed methodology, several nonlinear dynamical problems are addressed in section 5. Conclusions are drawn in section 6.

2. Original problem and considered dynamic regime

Consider a discrete, time-invariant, mechanical system whose dynamics is governed by a second-order ordinary differential equation (ODE),

$$\mathbf{M}\ddot{\mathbf{u}}(t) + \mathbf{f}(\mathbf{u}(t), \dot{\mathbf{u}}(t)) = -\tilde{\mathbf{K}}\mathbf{u} - \tilde{\mathbf{C}}\dot{\mathbf{u}} + \hat{\mathbf{f}}_e \frac{e^{i\phi_e(t)} + e^{-i\phi_e(t)}}{2}. \quad (1)$$

Herein, $\mathbf{M} = \mathbf{M}^T > 0$ is the real, symmetric, positive definite mass matrix and $\mathbf{u}(t)$ is the vector of generalized coordinates. The operator \mathbf{f} comprises nonlinear functions in displacement and velocity, and does not explicitly depend on time so that parametric excitation is excluded. $\tilde{\mathbf{K}}$ and $\tilde{\mathbf{C}}$ are symmetric linear stiffness and damping terms, respectively. $\hat{\mathbf{f}}_e$ and $\phi_e(t)$ represent amplitude vector and phase function of the external forcing.

Throughout this study, the considered dynamics are limited to the regime where nonlinear modal interactions are absent and the energy is confined in an isolated nonlinear mode. It is further assumed that the linear stiffness and damping terms on the right hand side of Eq. (1) are weak in the sense that they do not significantly deteriorate the geometry of the invariant manifold associated with the considered mode. A transient forcing can be taken into account in Eq. (1), but the phase function $\phi_e(t)$ is assumed to exhibit a dominant instantaneous frequency near the fundamental resonance of the considered mode. In accordance with the deformation-at-resonance property of nonlinear modes [22], it is therefore reasonable to assume that the external forcing only controls the amplitude but not the shape of the nonlinear mode. The damping matrix $\tilde{\mathbf{C}}$ may be indefinite so that self-excitation is possible in the absence of external forcing.

However, it is assumed that the damping matrix is positive if external forcing is present.

With these assumptions, it is possible to neglect the weak stiffness and damping terms on the right hand side of Eq. (1) for modal analysis step described in section 3 and to re-introduce these effects in ROM formulation in section 4. The motivation for this is to equip the ROM with a high-dimensional parameter space, since the parameters associated with external forcing, damping and stiffness are retained. This makes the proposed approach particularly attractive for exhaustive parametric studies. Furthermore, the modal analysis is simplified in this approach compared to approaches where forcing is taken into account in the modal analysis step, since the dimension of the phase space is reduced [3, 5, 4].

Instead of computing the nonlinear modes directly for the problem in Eq. (1), they are therefore computed for the autonomous surrogate problem Eq. (2),

$$\mathbf{M}\ddot{\mathbf{u}}(t) + \mathbf{f}(\mathbf{u}(t), \dot{\mathbf{u}}(t)) = \mathbf{0}. \quad (2)$$

In this study, the slow dynamics, i. e. the unsteady dynamics with a fast oscillation with slowly varying amplitude and phase is addressed.

3. Formulation and solution of the complex eigenvalue problem

As in a linear modal analysis, the problem Eq. (2) is solved using an exponential ansatz. In contrast to a linear system, however, the notion of eigenvectors is generalized so that the *eigenvectors* can comprise multi-harmonic content. Hence, $\mathbf{u}(t)$ is expressed in terms of the modal amplitude a and the complex components Ψ_n ,

$$\mathbf{u}(t) = a \operatorname{Re}\left\{ \sum_{n=0}^{N_h} \Psi_n e^{n\lambda t} \right\}. \quad (3)$$

Note that the generalized Fourier series is truncated to the harmonic order N_h . For a nonlinear system, all harmonics can be non-zero in general, including the zeroth-order term Ψ_0 which corresponds to a static offset. The formulation of Eq. (3) implies that the complex fundamental eigenfrequency λ is the same for

all harmonics. The undamped eigenfrequency ω_0 and the modal damping ratio D are related to λ as follows:

$$\lambda = -D\omega_0 + i\omega_0\sqrt{1 - D^2}. \quad (4)$$

The set $\{\lambda, \Psi_0, \dots, \Psi_{N_h}\}$ consisting of complex eigenfrequency and harmonic components is denoted eigenpair.

The eigenproblem is solved in the frequency domain. Therefore, the ansatz in Eq. (3) is substituted into Eq. (2) and subsequent Fourier-Galerkin projection yields a nonlinear system of algebraic equations. Similar to the linear case, amplitude and phase normalization constraints are imposed to make the number of equations equal to the number of unknowns. The resulting *complex eigenproblem* can be stated as:

$$\begin{aligned} &\text{solve} \quad (n\lambda)^2 \mathbf{M} \Psi_n a + \langle \mathbf{f}(\mathbf{u}_p, \dot{\mathbf{u}}_p), e^{in\omega_0 t} \rangle = \mathbf{0}, \quad n = 0 \dots N_h \\ &\text{subject to} \quad \underbrace{\Psi_1^H \mathbf{M} \Psi_1 = 1}_{\text{amplitude norm.}}, \quad \underbrace{\text{Re}\{\mathbf{t}^H \Psi_1\} = 0}_{\text{phase norm.}} \\ &\text{with respect to} \quad \{\lambda, \Psi_0, \dots, \Psi_{N_h}\}. \end{aligned} \quad (5)$$

The constant vector \mathbf{t} is used here to constrain the phase of the fundamental harmonic of the eigenvector Ψ_1 . The amplitude normalization to the mass matrix makes the formulation consistent with the classical formulation of the linear modal analysis.

An important aspect of the formulation in Eq. (5) is that the modal analysis involves the periodic forms of displacement \mathbf{u}_p , velocity $\dot{\mathbf{u}}_p$ instead of the pseudo-periodic ones in Eq. (3) as in [15, 16]. These periodic forms are defined as follows:

$$\mathbf{u}_p = a \text{Re}\left\{\sum_{n=0}^{N_h} \Psi_n e^{in\omega_0 t}\right\}, \quad \dot{\mathbf{u}}_p = a \text{Re}\left\{\sum_{n=0}^{N_h} in\omega_0 \Psi_n e^{in\omega_0 t}\right\}, \quad (6)$$

and the associated inner product

$$\langle c(\omega_0 t), d(\omega_0 t) \rangle = \frac{1}{2\pi} \int_{(2\pi)} c(\omega_0 t) \bar{d}(\omega_0 t) d\omega_0 t. \quad (7)$$

The strategy of using periodic formulations inherently allows for the direct calculation of periodic orbits and their associated harmonic decomposition. The computed nonlinear modes are therefore consistent with steady-state conditions. Since we are interested in dynamics with slowly increasing as well as decreasing energy, this approach gives rise to results that are centered with respect to energy.

The generalized Fourier coefficients $\langle \mathbf{f}(\mathbf{u}_p, \dot{\mathbf{u}}_p), e^{in\omega_0 t} \rangle$ of the nonlinear forces in Eq. (5) can typically not be expressed in closed-form and in general has to be evaluated numerically. Using periodic forms in the evaluation of the generalized Fourier coefficients facilitates the application of existing (high-order) harmonic balance formulations which require this periodicity. Available formulations exist for various conservative and non-conservative nonlinear systems (see e.g. [23, 24, 14, 25]) and shall not be repeated at this point.

The frequency-domain solution of the nonlinear eigenproblem can be regarded as a straight-forward extension of the linear eigenproblem. The governing algebraic system of equations can be solved using e.g. a Newton-Raphson method. Typically, the linearized eigenpair represents a valid and often good initial guess for small modal amplitudes. The efficiency of the solution process can be enhanced by using analytical gradients as proposed in [16]. An exact condensation of the algebraic system of equations can significantly reduce the required computational effort in case of sparse nonlinear operators [16] present e.g. in jointed structures. The solution of Eq. (5) has to be carried out for each nonlinear mode of interest in the relevant modal amplitude range.

The range of validity of the proposed reduction to a single nonlinear mode is limited to the regime where the considered nonlinear mode is stable and unique. Nonlinear modal interactions can lead to folds and bifurcations of nonlinear modes [16, 26, 14, 13]. Continuation with respect to the modal amplitude in conjunction with stability and bifurcation analysis can reveal these phenomena. Since the problem is formulated in the frequency domain, stability can be analyzed using Hill's theory [27, 28]. Alternatively, Floquet theory can be directly applied by computing and investigating the eigenvalues of the monodromy ma-

trix associated with the periodic orbits [29, 6, 20].

3.1. Definition of invariant manifolds

It should be noted that the phase normalization was only imposed in Eq. (5) in order to make the number of equations equal to the number of unknowns. In the autonomous case, the phase is generally arbitrary and an absolute phase ϑ can be introduced. Hence, the eigensolution can be generally written as

$$\begin{aligned} \mathbf{u} = \mathbf{P}(a, \vartheta) &:= a \frac{\mathbf{v} + \bar{\mathbf{v}}}{2}, \quad \dot{\mathbf{u}} = \mathbf{Q}(a, \vartheta) := \dot{\mathbf{P}}(a, \vartheta), \\ \text{with } \mathbf{v}(a, \vartheta) &= \sum_{n=0}^{N_h} \mathbf{\Psi}_n(a) e^{in\vartheta}. \end{aligned} \quad (8)$$

Clearly, Eq. (8) defines a two-dimensional invariant manifold in phase space, consistent with the invariant manifold concept developed by SHAW AND PIERRE[1]. The manifold is described in a polar coordinate system with the modal amplitude $a(t)$ and the absolute phase $\vartheta(t)$ which both can be arbitrary functions in time t . It should be remarked that the term \mathbf{Q} is only defined here for the sake of completeness of the phase space and the time derivative is not carried out at this point.

4. Prediction of the slow dynamics of the nonlinear mode

In accordance with the single nonlinear mode theory [30], the ROM in this study is restricted to the regime where nonlinear modal interactions are absent. If this assumption does not hold, a higher-dimensional ROM would have to be developed [4]. It should be recalled that the weak damping and stiffness terms, as well as the fundamental near-resonant forcing in Eq. (1) have to remain small enough in order to achieve accurate predictions with the ROM based on the nonlinear modes of the surrogate problem Eq. (2) in which these effects are neglected. Significant deviations are expected for fast transient phenomena, strong variation of the eigenvector due to the additional damping and stiffness terms and in situations where the system is driven into energy regimes featuring nonlinear modal interactions.

In order to derive the ODEs governing the slow dynamics on the manifold, the complexification-averaging technique [19] is employed. Therefore, a coordinate transform is defined,

$$\mathbf{u} := a \frac{\mathbf{v}(a, \vartheta) + \bar{\mathbf{v}}(a, \vartheta)}{2}, \quad \dot{\mathbf{u}} := ai\Omega \frac{\mathbf{v}(a, \vartheta) - \bar{\mathbf{v}}(a, \vartheta)}{2}. \quad (9)$$

The scalar complex variable conventionally introduced in the complexification-averaging process is here generalized to the multiharmonic vector \mathbf{v} as defined in Eq. (8). In Eq. (9), $\vartheta = \vartheta(t)$ is the time dependent phase of the mode and Ω is the frequency of oscillation.

The key point of the approximation is the decomposition into fast and slow dynamics, i. e. fast and slowly varying components of the phase $\vartheta(t)$,

$$\vartheta(t) = \underbrace{\phi(t)}_{\text{fast}} + \underbrace{\Theta(t)}_{\text{slow}}, \quad (10)$$

$$\Omega := \dot{\phi}(t). \quad (11)$$

The difference between the time scale of fast phase $\phi(t)$ and slow phase $\Theta(t)$ is assumed to be prominent, so that it is valid to approximate the angular frequency Ω by the time derivative of the fast phase.

The fast phase $\phi(t)$ corresponds to the eigenfrequency ω_0 in the autonomous case, and is assumed to be induced by excitation in the forced case,

$$\dot{\phi}(t) := \begin{cases} \omega_0 & \text{autonomous dynamics} \\ \dot{\phi}_e(t) & \text{non-autonomous dynamics} \end{cases}. \quad (12)$$

Subsequently, the classical averaging process can be carried out. A detailed derivation is given in appendix Appendix A. The resulting first order ODEs in a, Θ read

$$\begin{bmatrix} \dot{a} \\ \dot{\Theta} \end{bmatrix} = \frac{1}{2\Omega} \begin{bmatrix} -2\tilde{D}\tilde{\omega}_0\Omega a - \Psi_1^H \hat{\mathbf{f}}_e \sin \Theta \\ \tilde{\omega}_0^2 - \Omega^2 - \frac{1}{a} \Psi_1^H \hat{\mathbf{f}}_e \cos \Theta \end{bmatrix}. \quad (13)$$

Herein, the modified modal properties are defined as

$$\tilde{\omega}_0^2 = \omega_0^2 + \Psi_1^H \tilde{\mathbf{K}} \Psi_1, \quad 2\tilde{D}\tilde{\omega}_0 = 2D\omega_0 + \Psi_1^H \tilde{\mathbf{C}} \Psi_1. \quad (14)$$

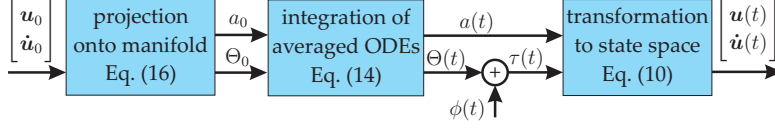


Figure 1: Overview of the proposed algorithm for the approximation of the slow dynamics of nonlinear modes

It should be emphasized that the modal properties $\omega_0(a)$, $D(a)$, $\Psi_1(a)$ depend on the modal amplitude a , turning Eq. (13) into a nonlinear problem.

The solution of Eq. (14) is particularly efficient in this formulation for two reasons: (1) The dimensionality of the problem is at maximum two, (2) the evaluation of the nonlinear terms in Eq. (14) does not involve the original possibly expensive nonlinear operator \mathbf{f} but only the readily available amplitude-dependent modal properties. This procedure therefore combines the highly accurate multiharmonic analysis of the full system subject to various, possibly strong nonlinearities, with the small and simple problem in Eq. (14).

In a numerical procedure, the modal properties will only be computed at discrete amplitude values. Hence, a one-dimensional interpolation scheme has to be used in order to apply the continuous formulation in Eq. (13) to the numerical results of the modal analysis.

Some special cases should be highlighted at this point: Under *steady-state* conditions $\dot{a} = 0 = \dot{\Theta}$, the ODE system in Eq. (13) degenerates to an algebraic system of equations in a, Θ , as already presented in [16]. Otherwise, Eq. (13) in conjunction with appropriate initial conditions $a(t=0) = a_0$, $\Theta(t=0) = \Theta_0$, represents an initial value problem that governs the slow dynamics of the considered system. In the *autonomous case*, the second line of Eq. (13) yields $\Theta = \Theta_0$ and the first line degenerates to $\dot{a} = \tilde{D}(a)\tilde{\omega}_0(a)a$.

4.1. Projecting the initial state onto the manifold

In a typical technical problem, the initial values for a, Θ are not a priori known, but rather the initial values are given in state space $\mathbf{u}_0, \dot{\mathbf{u}}_0$. In this paper, a closest point projection is proposed to find a suitable point on the manifold

corresponding to the actual initial state. This projection can be achieved by solving the following minimization problem,

$$a_0, \Theta_0 = \arg \min_{a, \Theta} \left\| \mathbf{u}_0 + \frac{1}{i\Omega} \dot{\mathbf{u}}_0 - a \mathbf{v}(a, \vartheta(\Theta)) \right\| \quad (15)$$

It is generally possible that the initial state does not exactly lie on the manifold. In this case, the energy is not confined to the nonlinear mode anymore which violates the fundamental assumption of the proposed ROM. Hence, agreement with the dynamic behavior of the original system cannot be assured.

An overview of the proposed methodology is presented in Fig. 1.

5. Numerical examples

The authors developed a software environment for the nonlinear modal analysis and ROMs for steady-state and transient predictions. Several nonlinear example problems have been studied. The first examples in subsections 5.1-5.2 are single and two DOF examples, respectively, and aim at demonstrating the capabilities of the proposed method regarding complex problems in detail. The last example in subsection 5.3 is a FE model of a beam with friction contact and is designated to highlight the beneficial numerical performance that can be achieved by using the ROM. The results of the ROM are generally compared to the results obtained from direct time integration of the original system.

5.1. Single degree-of-freedom systems

5.1.1. Duffing oscillator

The dynamics of an autonomous, linearly damped Duffing oscillator are investigated. The associated initial value problem reads

$$\ddot{u}(t) + 2d\dot{u}(t) + u(t) + k_{\text{nl}}u^3(t) = 0, \quad u(0) = u_0, \dot{u}(0) = 0. \quad (16)$$

For this problem, a closed-form analytical approximation can be easily obtained by means of averaging [31],

$$u(t) \approx u_0 e^{-dt} \cos \left(t + 3k_{\text{nl}}u_0^2 \frac{e^{-2dt} - 1}{16} \right). \quad (17)$$

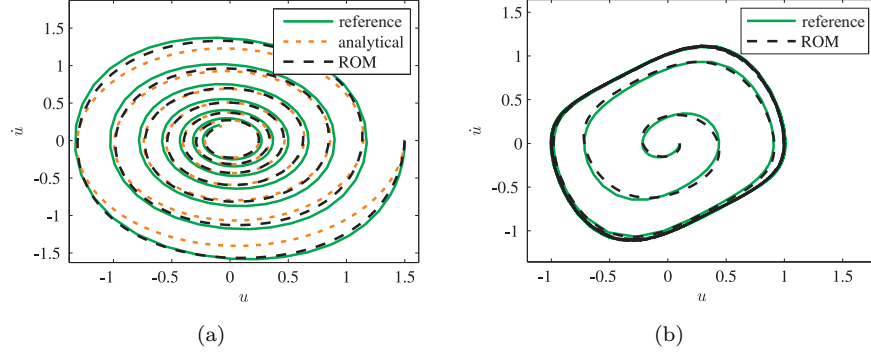


Figure 2: Phase portraits of autonomous single degree-of-freedom systems ((a) Duffing oscillator with linear damping, $d = 0.05$, $k_{nl} = 0.25$, $u_0 = 1.5$, (b) Van der Pol oscillator, $\alpha = 0.5$, $\beta = 2, u_0 = 0.1$)

This analytical solution is compared to the proposed ROM and the direct time integration results in the phase portrait in Fig. 2a. It can be seen that the accuracy of the ROM is significantly better than the analytical approximation for large amplitudes. All three methods agree well for smaller amplitudes. Slight deviations from the numerically computed reference solution can be explained by the error introduced by averaging.

5.1.2. Van der Pol oscillator

Next, the autonomous Van der Pol oscillator is considered. The initial value problem governing the autonomous dynamics can be stated as

$$\ddot{u}(t) - (\alpha - \beta u^2(t)) \dot{u}(t) + u(t) = 0, \quad u(0) = u_0, \dot{u}(0) = 0. \quad (18)$$

In contrast to the previous example, the attractor is not a fixed point but a periodic orbit known as limit cycle, see Fig. 2b. Again, the results obtained by the ROM are in excellent agreement with the reference method. Owing to the synthesis of all harmonics contributing to the eigenvector in Eq. (8), the apparent multiharmonic character of the limit cycle is well-captured.

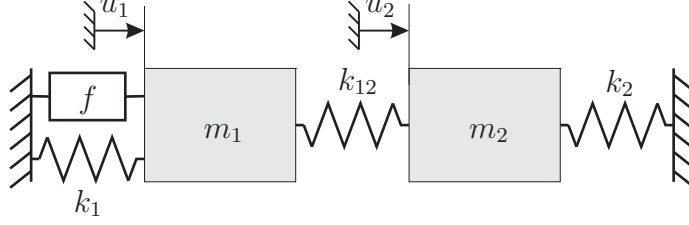


Figure 3: Two degree-of-freedom system with nonlinear element

5.2. Two degree-of-freedom systems

In this subsection, a two DOF model is considered. It consists of two masses and three linear springs, as illustrated in Fig. 3. The effect of different nonlinear forces f acting on one of the masses and stemming from either a cubic spring, a Coulomb friction element or a unilateral spring, is investigated in the following. If not otherwise specified, the results are illustrated for the displacement u_2 . Amplitude-dependent modal properties are illustrated with respect to the modal amplitude a_2 defined as the fundamental harmonic amplitude of u_2 , i. e. $a_2 = |a\Psi_{1,2}|$. For the sake of clarity in the figures, many results of the ROM are only depicted in terms of the envelope.

5.2.1. Cubic spring nonlinearity

In case of the nonlinear spring with stiffness k_{nl} , the force f reads

$$f = k_{nl}u_1^3. \quad (19)$$

The so called Frequency-Energy-Plot is depicted for the first mode in Fig. 4. Nonlinear modal interactions with the second mode can be recognized in the form of tongues in Fig. 4 [26]. Not only the frequency increases with the modal amplitude, but also the mode shape varies. For the points marked by a cross, the mode shape is illustrated in Fig. 4 in the $u_2 - u_1$ plane. It can be seen that the mode shape becomes nonlinear as the modal amplitude increases and finally localizes in the right mass in Fig. 3. The interested reader is referred to [26] for a comprehensive stability and bifurcation analysis of this system.

We now focus on the transient, autonomous dynamics of this system. To this

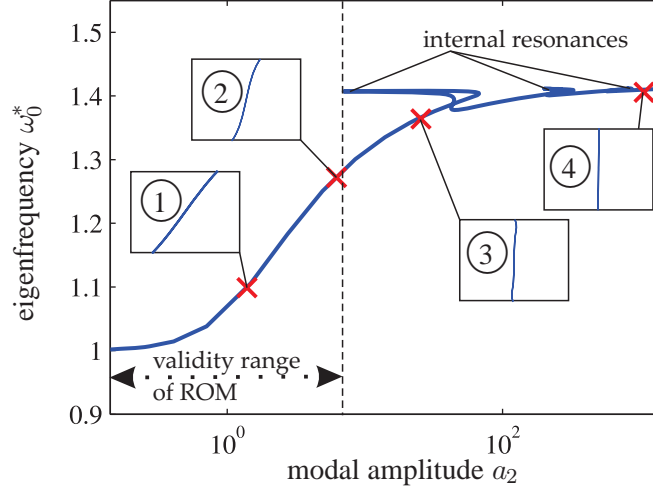


Figure 4: Frequency-energy plot of the first nonlinear mode of the system with cubic spring, subfigures represent phase projections in the $u_2 - u_1$ plane, $m_1 = m_2 = 1$, $k_1 = k_2 = k_{12} = 1$, $k_{nl} = 0.5$

end, a constant, mass-proportional damping $\tilde{\mathbf{C}} \propto \mathbf{M}$ is specified. The magnitude of the damping term will be provided in terms of a linear (i.e. for $f = 0$) modal damping ratio.

In Figs. 5, the time histories of both masses are illustrated for different initial modal amplitude values (and therefore also mode shape) corresponding to the points indicated in Fig. 4. The dynamics of the left mass (u_1) appear to be distorted beyond the modal amplitude value where the first bifurcation of the nonlinear mode occurs. This behavior cannot be predicted by the single modal ROM followed in this study. As expected, the ROM is restricted to modal amplitude regimes where the nonlinear modes do not interact with each other [26, 18]. However, the envelope of the displacement u_2 of the right mass is in excellent agreement with the reference simulation. This applies even for large initial modal amplitudes, i.e. regardless of the presence of nonlinear modal interactions.

In Fig. 6, the time histories are depicted for the same initial modal amplitude (before the bifurcation point) but different damping values. Again, good

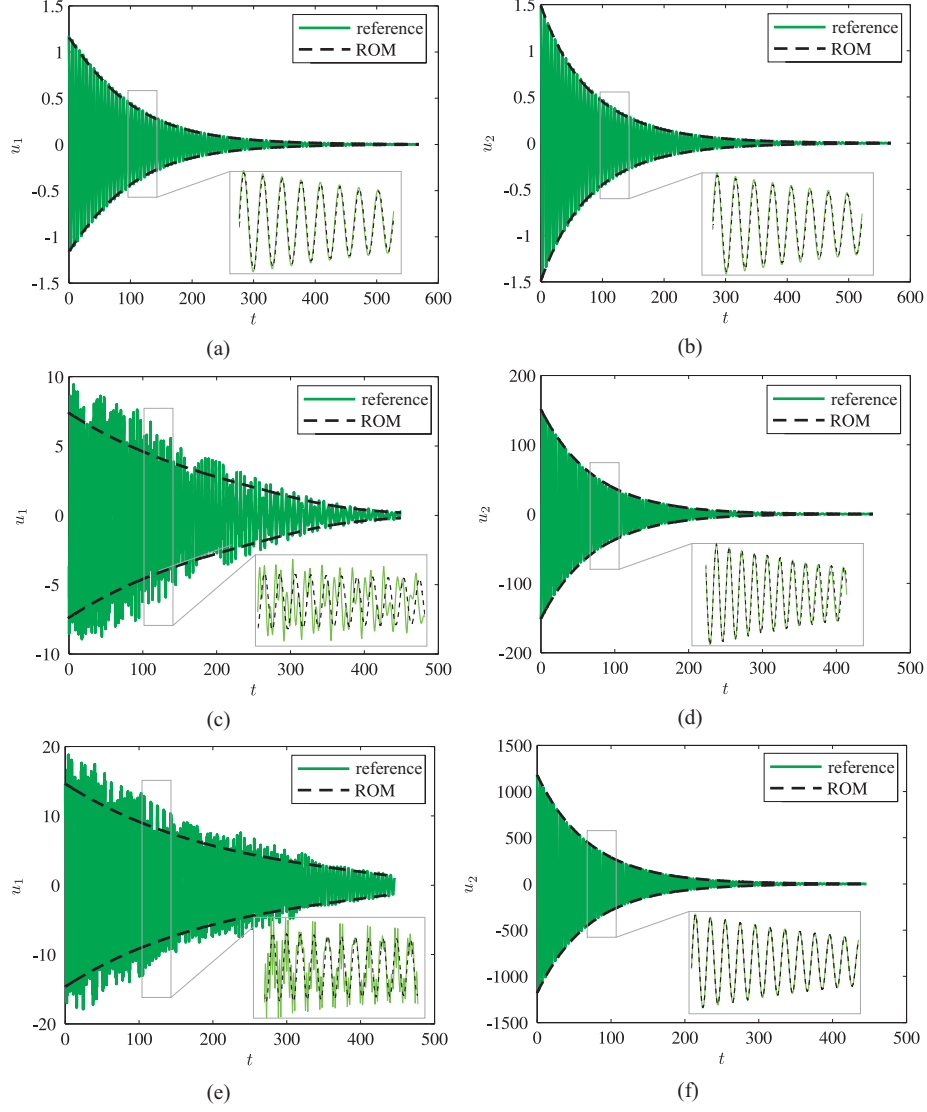


Figure 5: Time histories of autonomous system with cubic spring, 1% damping ratio ((a) u_1 for starting point ①, (b) u_2 for starting point ①, (c) u_1 for starting point ③, (d) u_2 for starting point ③, (e) u_1 for starting point ④, (f) u_2 for starting point ④)

agreement between the ROM and the reference results can be ascertained, in particular for displacement u_2 . The consideration of the effect of damping on the modal properties in the ROM according to Eq. (14) can therefore be regarded

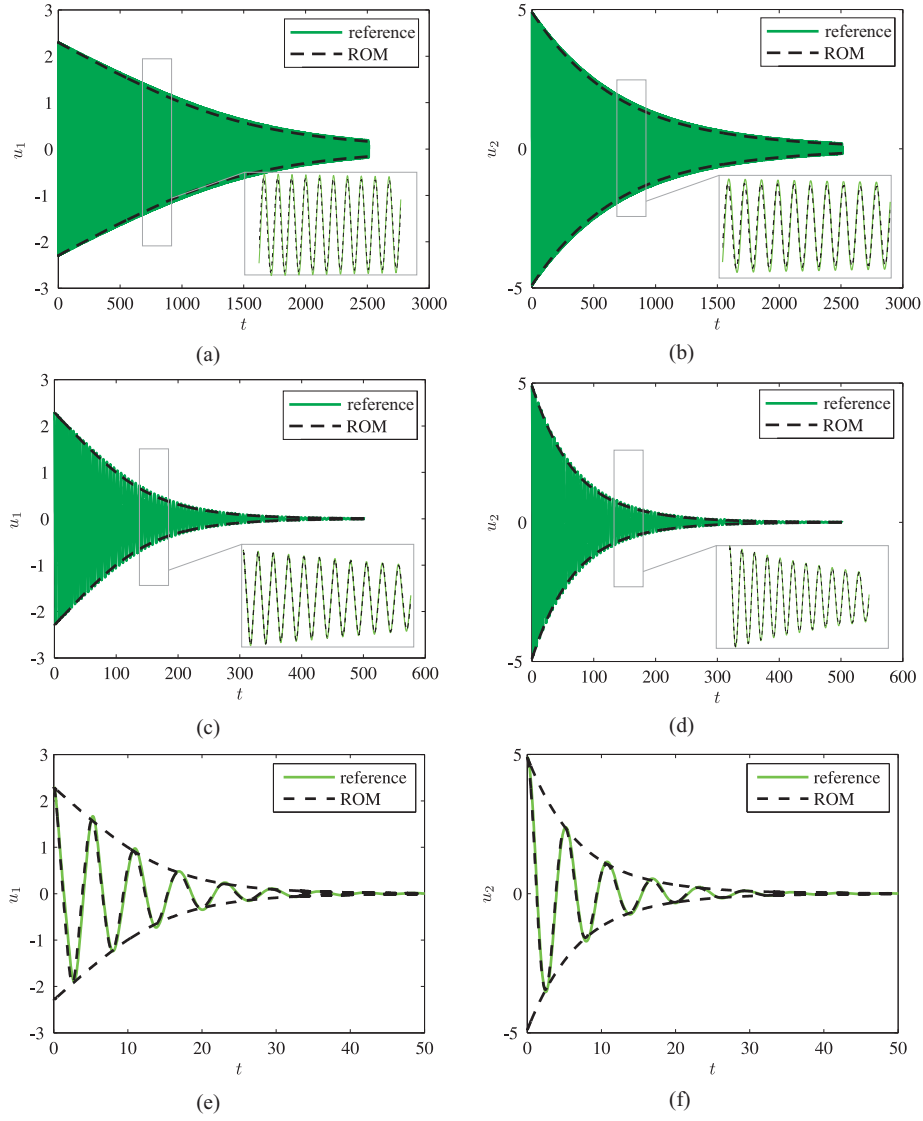


Figure 6: Time histories of autonomous system with cubic spring, starting point $\textcircled{2}$ ((a) u_1 for 0.1% damping ratio, (b) u_2 for 0.1% damping ratio, (c) u_1 for 1% damping ratio, (d) u_2 for 1% damping ratio, (e) u_1 for 10% damping ratio, (f) u_2 for 10% damping ratio)

as valid for this example, even for damping ratios as large as 10%.

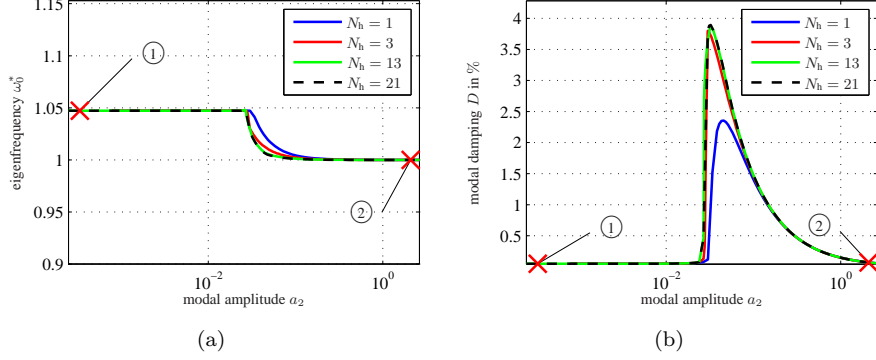


Figure 7: Nonlinear modal properties of first mode of system with friction nonlinearity, $m_1 = 0.02$, $m_2 = 1$, $k_1 = 0$, $k_{12} = 40$, $k_2 = 600$, $R = 1$, $\varepsilon = 0.01$ ((a) eigenfrequency, (b) modal damping)

5.2.2. Coulomb friction nonlinearity

The cubic spring is now replaced by a Coulomb friction element. The nonlinear force characteristic is defined as follows,

$$f = R \tanh\left(\frac{\dot{x}_1}{\varepsilon}\right). \quad (20)$$

Herein, R is the limit friction force and ε is a small regularization parameter determining the accuracy of the approximation of the signum function actually contained in the Coulomb law $f = R \operatorname{sgn} \dot{x}_1$. It should be pointed out that the modal analysis results depicted with scaled a/R axis are identical for any limit friction force value R [17, 16]. This scaling property allows for a straightforward extension of the ROM parameter space at no extra computational cost.

In Figs. 7a-7b, eigenfrequency and modal damping are illustrated for the first nonlinear mode of the system. The system exhibits two linear limit cases: For low amplitudes, the friction contact is fully stuck so that $u_1 = 0$. For very large amplitudes, the friction contact is always sliding. The limited friction force, however, has decreasing effect on the dynamic properties for large amplitudes so that the modal properties approach the values corresponding to the system without friction element. Note that a moderate harmonic order N_h is

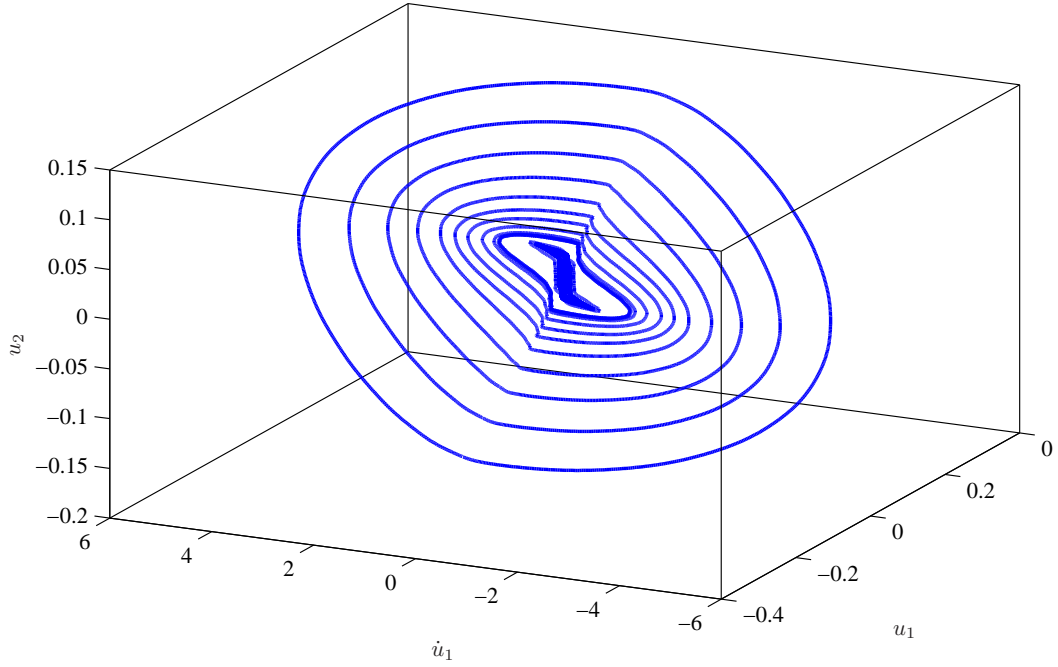


Figure 8: Manifold of first mode of system with friction nonlinearity

required to accurately capture the friction effect on this system. The multiharmonic character of the eigenmode also becomes apparent in the manifold plot in Fig. 8. The abrupt changes between stick and slip motion make the mode shapes significantly deviating from elliptic orbits. Furthermore, the mode shape significantly varies with the modal amplitude.

The two-mass system with friction element is only investigated in the forced configuration, for an autonomous system subject to friction, see subsection 5.3. In Figs. 9a- 9b, the time histories are illustrated for the case of steady forcing with near-resonant excitation frequency. Two different initial conditions are considered: In Fig. 9a, the system starts from its equilibrium point, while it starts from a modal amplitude larger than the steady-state amplitude in Fig. 9b.

Beating phenomena occur in both cases before reaching the steady-state with a constant amplitude. According to expectations, the frequency of this beating is smaller in Fig. 9b than it is in Fig. 9a since eigenfrequency and excitation

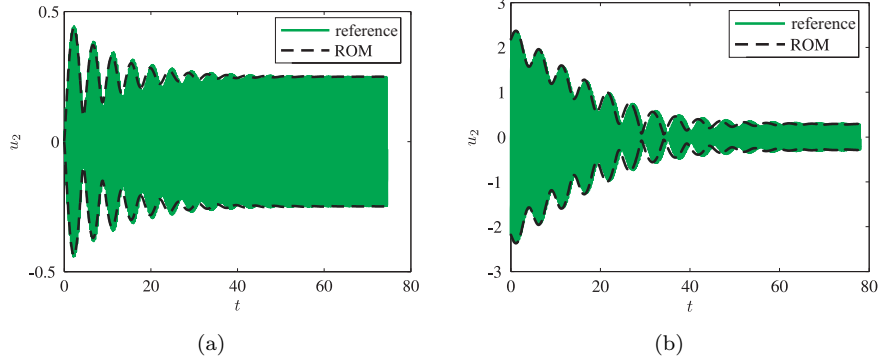


Figure 9: Time histories of system with friction nonlinearity subject to steady-state harmonic forcing ((a) frequency $\Omega = 0.9\omega_0$ ($a = 0$), starting point ①, (b) frequency $\Omega = 0.95\omega_0$ ($a = 0$), starting point ②)

frequency are closer in the first case. Dissipation due to friction and linear damping is the reason for the decay of the pulsation of the envelope part of the solution and the transition to the limit cycle. The amplitude of the limit cycle depends on the excitation level. Despite the initial energy of zero, it can be seen in Fig. 9a that the amplitude overshoots the steady-state amplitude before reaching the limit cycle. The slow flow results agree well with the direct time integration results for both steady cases, in spite of the strongly nonlinear system behavior.

In Fig. 10, the time histories are depicted for the case of a sine sweep, i. e. quasi-harmonic forcing with linearly increasing excitation frequency. In all three cases the system dynamics are specified to start from the equilibrium point.

Again, a pulsation phenomenon occurs in the response, which is accurately captured by the proposed approximation method. The maximum amplitude of the first pulse decreases with increasing angular acceleration. The excitation frequency at this maximum amplitude apparently increases with increasing angular acceleration. In case of the largest frequency acceleration in Fig. 10(c), the eigenfrequency of the second mode is reached within the depicted time span. In full accordance with the restriction of the ROM, the dynamics are

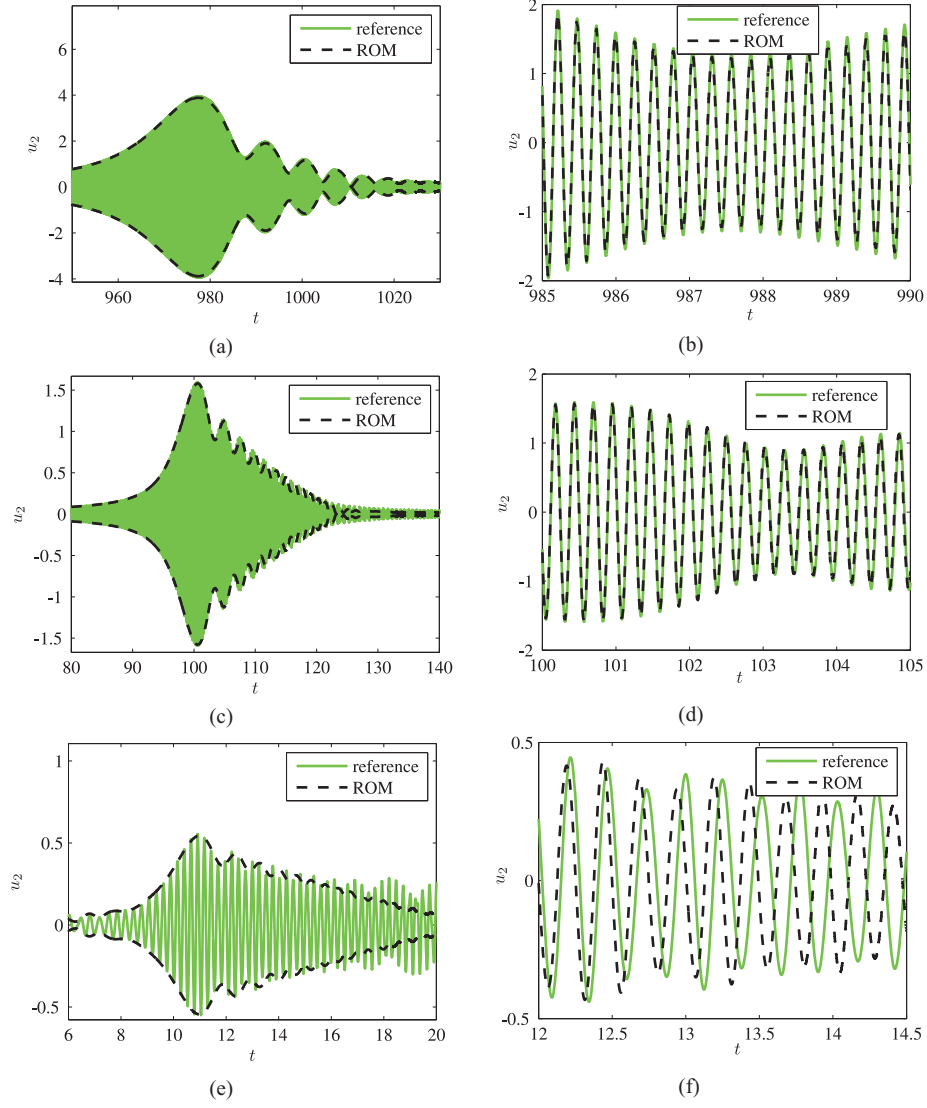


Figure 10: Time histories of system with friction nonlinearity subject to a sine sweep ((a) and (b) $\dot{\phi}_e(t) = 0.025 t$, (c) and (d) $\dot{\phi}_e(t) = 0.25 t$, (e) and (f) $\dot{\phi}_e(t) = 2.5 t$)

only predicted accurately in the vicinity of the eigenfrequency of the considered nonlinear mode, i.e. the first mode in this case. It is assumed that the accuracy of the proposed method could be improved in this case by simply superimposing the ROMs for both nonlinear modes. This has, however, not been done in the

present study. It should be noted that the maximum amplitude in the near the first resonance, which is typically of importance for design considerations, is accurately predicted by the ROM.

5.2.3. Unilateral spring nonlinearity

Next, the effect of a unilateral spring on the dynamics of the system in Fig. 3 is investigated. The unilateral spring of stiffness k_{nl} is considered to be preloaded by a constant force N so that the nonlinear force reads

$$f = \begin{cases} -N & k_{nl}u_1 < -N \\ k_{nl}u_1 & k_{nl}u_1 \geq -N \end{cases}. \quad (21)$$

Eigenfrequency and manifold of the second nonlinear mode are depicted in Figs. 11a-11b. Note that since the system is conservative, the nonlinear modal damping is identical to zero and therefore not depicted. As soon as the amplitudes are large enough, the preload is exceeded so that the spring undergoes lift-off during the period of oscillation. As a consequence, the nonlinear mode becomes asymmetrical to the origin. This can be easily deduced from Fig. 11b. It is thus essential to not only account for the higher harmonics but also to consider the zeroth harmonic of the nonlinear mode.

The system is first investigated in the autonomous configuration. Starting from a moderate initial amplitude as indicated in Fig. 11a, the system approaches its fix point as illustrated in the time histories in Fig. 12. A constant, mass-proportional damping has been specified such that all modes have a damping ratio of 1% in the linearized case. The effect of the stiffness term $\tilde{\mathbf{K}}$ in the ROM is investigated.

In the case $\tilde{\mathbf{K}} = \mathbf{0}$, the proposed method is in excellent agreement with the direct time integration, see upper two images in Fig. 12. Note the asymmetrical upper and lower envelope of the response. In accordance with the manifold in Fig. 11b, there is an offset such that the mean value of u_2 is negative in the region of partial lift-off. As the amplitude decreases due to the linear damping, the relative mean value decreases and finally vanishes as the lift-off phases be-

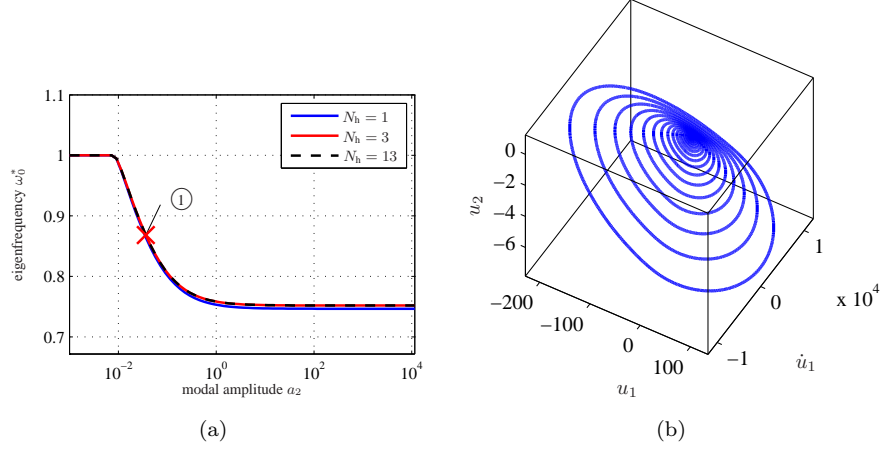


Figure 11: Nonlinear modal properties of second mode of system with unilateral spring, $m_1 = 0.02$, $m_2 = 1$, $k_1 = 0$, $k_{12} = 40$, $k_2 = 600$, $N = 1/70$, $k_{nl} = 70$ ((a) eigenfrequency, (b) manifold)

come shorter within one cycle of oscillation and finally vanish.

In case of nonzero stiffness terms $\tilde{\mathbf{K}} \neq \mathbf{0}$, the response appears to be distorted, see lower four images in Fig. 12. It is assumed that this distortion mainly results from the fact that the initial state is not precisely on the invariant manifold of the perturbed system. The averaged results can therefore only approximate the mean envelope in this case.

In Figs. 13a- 13b, the transient dynamics of the system subject to a sine sweep is illustrated. Once more, a very good agreement between proposed approximation and the direct time integration can be stated in the vicinity of the first eigenfrequency.

The asymmetrical character with respect to amplitude is again induced by the unilateral nonlinearity can easily be seen from the results. Similar to the results in Fig. 10(c), the ROM fails in predicting the ‘blast’ occurring at large times in Fig. 13b. Here, the excitation frequency reaches the eigenfrequency of the first mode and drives the mode into resonance. Since only the second mode was considered in the ROM, this phenomenon is not predicted.

It is noteworthy that there exists a strong qualitative discrepancy between

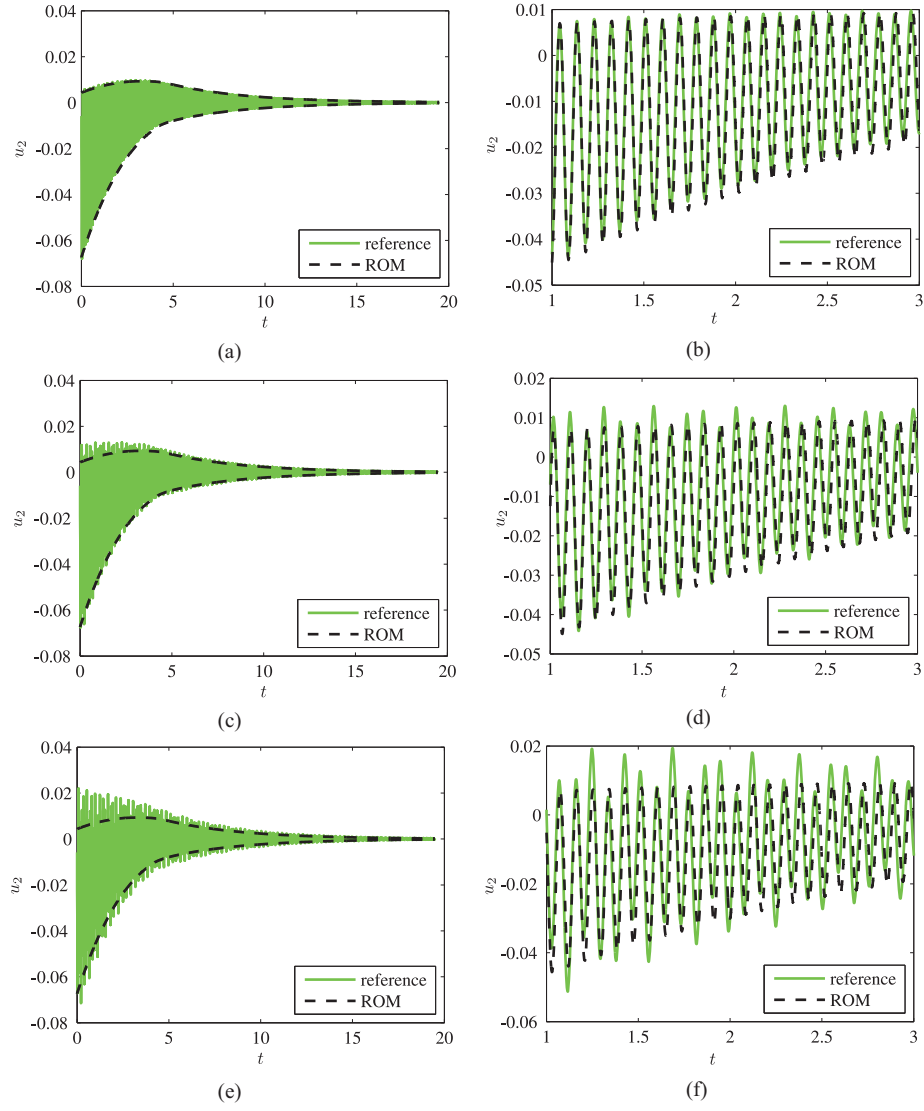


Figure 12: Time history of autonomous system with unilateral spring, starting point $\textcircled{1}$ ((a) and (b) $\tilde{\mathbf{K}} = \mathbf{0}$, (c) and (d) $\tilde{\mathbf{K}} = 0.1 \mathbf{K}$, (e) and (f) $\tilde{\mathbf{K}} = 0.25 \mathbf{K}$)

Fig. 13a and Fig. 13b. This discrepancy is not only caused by the deviation in the magnitude but also the sign of the angular acceleration. A typical frequency response curve of a system with unilateral preloaded spring is bent to the left such that there exists a frequency range with a multi-valued response.

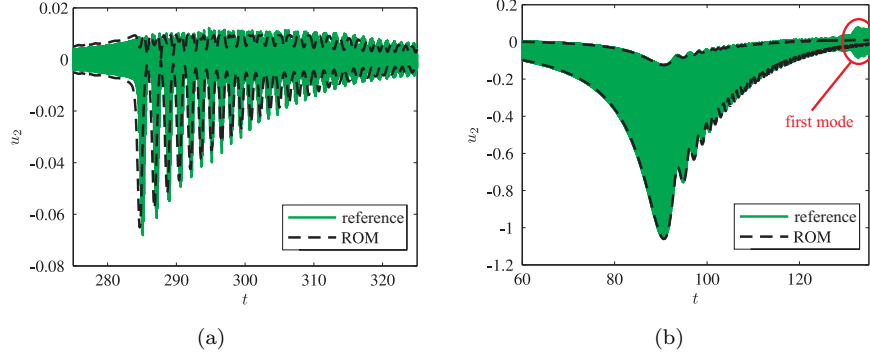


Figure 13: Time history of system with unilateral spring subject to a sine sweep ((a) $\dot{\phi}_e(t) = 0.25 t$, (b) $\dot{\phi}_e(t) = 1.75\omega_0(a = 0) - 0.025 t$)

Hence, the results for a down-sweep generally deviate from those of an up-sweep. Starting from a subcritical (supercritical) frequency, a jump phenomenon occurs when the frequency is increased (decreased) beyond the folding point of the frequency response curve. Comparatively fast amplitude changes can also be observed from Figs. 13a- 13b. However, the jump is not severe in this case due to the finiteness of the angular acceleration.

5.3. Beam with friction nonlinearity

A clamped beam with friction nonlinearity at single node at its free end has been investigated, see Fig. 14. The geometry was spatially discretized by means of solid Finite Elements. The original model comprised 3366 nodes and 9900

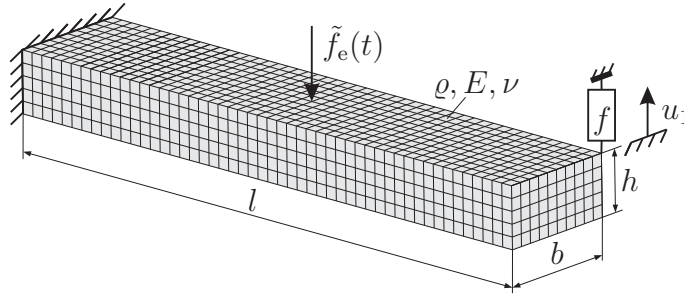


Figure 14: Cantilevered beam with nonlinear element subject to excitation

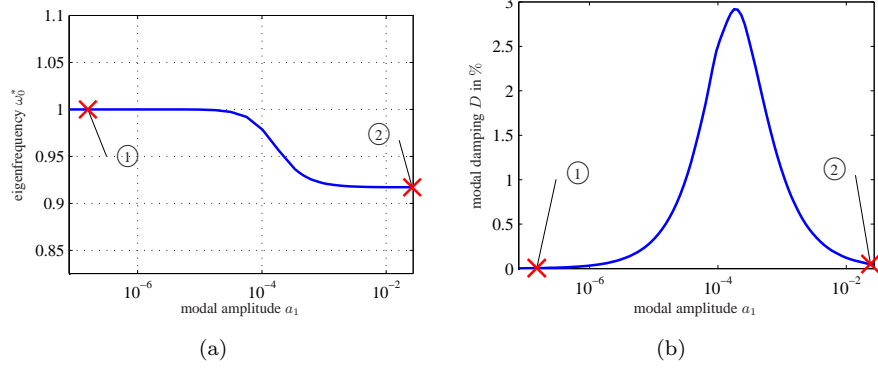


Figure 15: Nonlinear modal properties of first bending mode of beam with friction nonlinearity, $\rho = 4430 \text{ kg/m}^3$, $E = 100 \text{ GPa}$, $\nu = 0.3$, $l = 1 \text{ m}$, $b = 0.2 \text{ m}$, $h = 0.1 \text{ m}$, $k_t = 1 \text{ kN/mm}$, $R = 100 \text{ N}$, $\alpha = 1$ ((a) eigenfrequency, (b) modal damping)

DOFs. The Craig-Bampton technique was used to reduce the order of the underlying linear model. The first bending mode was studied. In accordance with a preliminary convergence study, the system dynamics are accurately described in the reduced basis composed of the static constraint mode of the nonlinear DOF and the first five fixed interface normal modes.

The Dahl friction model [32] is considered. The nonlinear friction force is governed by a differential equation,

$$\dot{f} = k_t \left(1 - \frac{f}{R} \text{sgn} \dot{u}_1 \right)^\alpha \dot{u}_1. \quad (22)$$

Herein, k_t is the initial slope of the hysteresis, R is the limit friction force and α is a parameter determining the shape of the hysteresis.

In Figs. 15a-15b, eigenfrequency and modal damping are depicted for the first mode of the system. The modal amplitude a_1 defined as the fundamental harmonic amplitude of the displacement u_1 of the contact node, i.e. $a_1 = |a\Psi_{1,1}|$. The results are generally similar to the ones obtained for the two DOF system with Coulomb nonlinearity, see Figs. 7a-7b. Since the Dahl model also describes the microslip behavior, the modal properties are smoother compared to results for the Coulomb macroslip model.

The system is first considered in the autonomous configuration without exter-

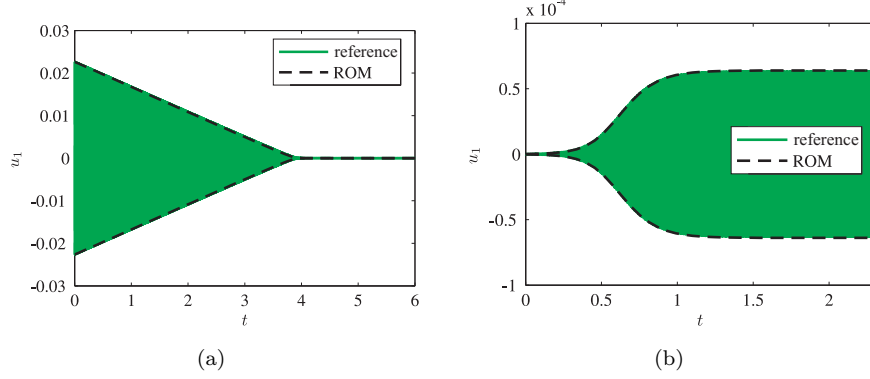


Figure 16: Time history of autonomous beam with friction nonlinearity ((a) transition to equilibrium with $\tilde{\mathbf{C}} = \mathbf{0}$ from starting point (1), (b) transition to limit cycle with $\tilde{\mathbf{C}} = \tilde{\mathbf{C}}_{-2\%}$ from starting point (2))

nal forcing. In the time history in Fig. 16a, the transient dynamics towards the equilibrium point are depicted. The well-known linear amplitude decay can be clearly deduced from the results.

The effect of aerodynamic instabilities such as flutter on the vibration behavior of nonlinear mechanical structures can be approximately described by an indefinite linear damping matrix [33, 17]. This can result in so called flutter-induced limit cycle oscillations. In this case, a constant damping matrix $\tilde{\mathbf{C}}_{-2\%}$ has been specified in such a way that the linearized system has a negative damping ratio of -2% for the first mode and a positive damping ratio of 1% for the remaining modes. The transition from zero amplitude to a stable limit cycle is depicted in Fig. 16b. Again, the results of the proposed ROM for the autonomous system are in excellent agreement with the direct time integration results.

The system is next considered in the heteronomous configuration with a sine sweep excitation. The time histories for two different frequency acceleration values are depicted in Figs. 17a- 17b. The results are generally in very good agreement. According to expectations, the agreement is slightly worse for considerably large frequency acceleration values, i. e. when the fast and slow phase have similar time scales. However, the time and amplitude of the largest peak

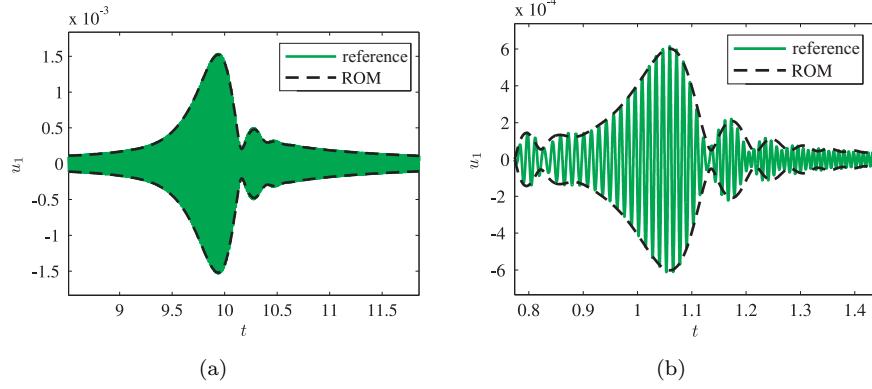


Figure 17: Time history of beam with friction nonlinearity subject to a sine sweep ((a) slow run-up, $\dot{\phi}_e(t) = 50 t$, (b) fast run-up, $\dot{\phi}_e(t) = 500 t$)

as well as the qualitative modulation behavior is captured well by the proposed ROM.

Table 1: Computational effort for conventional and proposed methodology

Problem	ODE dim. (direct)	CPU time (direct)	ODE dim. (ROM)	CPU time (ROM)
autonomous (Fig. 16a)	13	89 s	1	0.1 s
autonomous (Fig. 16b)	13	13 s	1	0.1 s
forced (Fig. 17a)	13	104 s	2	2.2 s
forced (Fig. 17b)	13	14 s	2	0.7 s

The computational effort required by the ROM is compared to the direct time integration of the original system in Tab. 1. The problem dimension of the original system is two times the number of retained generalized DOFs plus one dimension for the differential equation governing the friction effect in Eq. (22), i.e. the system dimension is $2 \cdot 6 + 1 = 13$. In case of the ROM the problem dimension is two (amplitude a and slow phase Θ) in the heteronomous case and one (amplitude a) in the autonomous case.

It can be easily ascertained from Tab. 1 that the computational effort to obtain

the time histories presented in this subsection can significantly be reduced by the proposed ROM. Not only the decreased problem dimension contributes to a reduction of the computational effort but also the averaging approach itself facilitates larger time steps in the integration process: The governing differential equations in Eq. (13) are formulated in the apparently more slowly varying coordinates and also the involved nonlinear terms are typically smoother compared to the ones involved in the original problem.

6. Conclusions

A novel method for the numerical computation of the slow dynamics of nonlinear mechanical systems has been developed. The method consists of a two-step procedure: In the first step, a multiharmonic analysis of the autonomous system is performed to directly compute the amplitude-dependent characteristics of the considered nonlinear mode. In the second step, these modal properties are used to construct a two-dimensional reduced order model (ROM). The numerical examples showed that the proposed ROM can be applied to various problems including strongly nonlinear conservative as well as non-conservative mechanical systems. The ROM is capable of directly calculating steady-state and approximating the slow dynamics of these systems in autonomous and heteronomous configurations provided that the vibration energy is confined to an isolated nonlinear mode. Moreover the ROM features a large parameter space including additional linear damping, stiffness and near-resonant forcing terms. The proposed concept reduces the gap between often studied academic single-degree-of-freedom and industrial FE models for nonlinear dynamical problems. It is believed that the ROM developed in this study represents a good basis for many multiphysics and multi-component problems, where the ROM is used to describe the structural dynamics of specific components. Further, the successful prediction of unsteady dynamics such as the energy decay of nonlinear modes is regarded as a corner stone for experimental nonlinear modal analysis of dissipative systems.

Future work should include the extension of the proposed ROM to problems where modal interactions of a finite number of nonlinear modes occur. Moreover, an error estimation of the ROM compared to the original model is highly desirable. In particular, the error induced by damping and stiffness terms that are only considered in the ROM, or starting points that lie outside the invariant manifold should be investigated in more detail.

Appendix A. Derivation of the averaged equations governing the slow dynamics of a nonlinear mode

In order to apply the complexification-averaging technique to Eq. (1), the acceleration $\ddot{\mathbf{u}}(t)$ has to be expressed in terms of the complex function $a\mathbf{v}$. This can be achieved by noting that $a\mathbf{v} = \mathbf{u} + \frac{\dot{\mathbf{u}}}{i\Omega}$ from Eq. (9) and taking the derivative with respect to time:

$$a\mathbf{v} = \mathbf{u} + \frac{\dot{\mathbf{u}}}{i\Omega} \quad (\text{A.1})$$

$$\Rightarrow (\dot{a\mathbf{v}}) = \dot{\mathbf{u}} + \frac{\ddot{\mathbf{u}}}{i\Omega} \quad (\text{A.2})$$

$$\Rightarrow \ddot{\mathbf{u}} = i\Omega \left((\dot{a\mathbf{v}}) - \dot{\mathbf{u}} \right). \quad (\text{A.3})$$

The time derivative $(\dot{a\mathbf{v}})$ is computed from Eqs. (8) and (11), taking into account the variation of the slow phase $\dot{\Theta}$ and amplitude \dot{a} ,

$$(\dot{a\mathbf{v}}) = \sum_{n=0}^{N_h} \Psi_n e^{in\vartheta} \left(\dot{a} + in \left(\Omega + \dot{\Theta} \right) a \right) + \underbrace{\frac{\partial \Psi_n}{\partial a} \dot{a} a e^{in\vartheta}}_{\approx 0}. \quad (\text{A.4})$$

The term associated with the sensitivity of the eigenvector and the slow variation of the amplitude is considered a second-order effect and therefore neglected in this study. By substituting Eq. (A.4) and the second equation in Eq. (9) into Eq. (A.3), one obtains the final form of Eq. (A.5):

$$\ddot{\mathbf{u}} = a\Omega^2 \frac{\mathbf{v} - \bar{\mathbf{v}}}{2} + \sum_{n=0}^{N_h} \Psi_n e^{in\vartheta} \left(i\Omega \dot{a} - n\Omega \left(\Omega + \dot{\Theta} \right) a \right). \quad (\text{A.5})$$

Eqs. (A.5) and (9) are then substituted into the original equation of motion in Eq. (1),

$$M\ddot{\mathbf{u}} + \mathbf{f} = \boldsymbol{\varepsilon}, \quad (\text{A.6})$$

with the function ε defined as,

$$\varepsilon(\mathbf{u}, \dot{\mathbf{u}}, t) = -\tilde{\mathbf{K}}\mathbf{u} - \tilde{\mathbf{C}}\dot{\mathbf{u}} + \hat{\mathbf{f}}_e \frac{e^{i\phi_e(t)} + e^{-i\phi_e(t)}}{2}. \quad (\text{A.7})$$

Functional dependencies are dropped for the sake of brevity in Eq. (A.6). The resulting equation is then projected onto the fundamental harmonic of the nonlinear mode $\Psi_1 e^{i\vartheta}$. Therefore, the inner product $\Psi_1^H \langle \cdot, e^{i\vartheta} \rangle$ as defined in Eq. (7) is applied to Eq. (A.6). The individual terms obtained by this projection read

$$\Psi_1^H \langle \mathbf{M}\ddot{\mathbf{u}}, e^{i\vartheta} \rangle = i\Omega\dot{a} - \frac{\Omega^2}{2}a - \dot{\Theta}\Omega a, \quad (\text{A.8})$$

$$\Psi_1^H \langle \mathbf{f}, e^{i\vartheta} \rangle = \frac{\omega_0^2}{2}a + D\omega_0 i\Omega a, \quad (\text{A.9})$$

$$\Psi_1^H \langle \varepsilon, e^{i\vartheta} \rangle = -\frac{\Psi_1^H \tilde{\mathbf{K}} \Psi_1}{2}a - \frac{\Psi_1^H \tilde{\mathbf{C}} \Psi_1}{2}i\Omega a + \frac{\Psi_1^H \hat{\mathbf{f}}_e}{2}e^{-i\Theta}. \quad (\text{A.10})$$

Herein, the normalization constraint in Eq. (5), $\Psi_1^H \mathbf{M} \Psi_1 = 1$, was taken into account. The projection of the nonlinear force \mathbf{f} is expressed in terms of the modal properties of the corresponding nonlinear mode in full accordance with Eq. (5). This approximation of the nonlinear forces is the key aspect for the efficient ROM since the often expensive nonlinear operator does not have to be evaluated in ROM, but the readily available modal properties are considered instead.

By substituting the projected terms in Eq. (A.10) into Eq. (A.6) and equating real and imaginary parts, one finally arrives at the ODE system in Eqs. (13) and (14).

It is interesting to note that only the complex eigenfrequency and the fundamental harmonic Ψ_1 of the eigenvector occurs in Eq. (13). Due to the nonlinear character of Eq. (5), these results are coupled to the remaining harmonic components Ψ_n and generally differ from the results of a single-harmonic analysis.

References

- [1] S. W. Shaw, C. Pierre, Normal Modes for Non-Linear Vibratory Systems, Journal of Sound and Vibration 164 (1) (1993) 85–124.

- [2] A. H. Nayfeh, *Nonlinear Interactions: Analytical, Computational and Experimental Methods*, John Wiley & Sons, 2000.
- [3] D. Jiang, C. Pierre, S. W. Shaw, Nonlinear normal modes for vibratory systems under harmonic excitation, *Journal of Sound and Vibration* 288 (4-5) (2005) 791–812.
- [4] C. Pierre, D. Jiang, S. W. Shaw, Nonlinear normal modes and their application in structural dynamics, *Mathematical Problems in Engineering* 10847 (2006), 1–15.
- [5] C. Touzé, M. Amabili, Nonlinear normal modes for damped geometrically nonlinear systems: Application to reduced-order modelling of harmonically forced structures, *Journal of Sound and Vibration* 298 (4–5) (2006) 958–981.
- [6] D. Jiang, C. Pierre, S. W. Shaw, Large-amplitude non-linear normal modes of piecewise linear systems, *Journal of Sound and Vibration* 272 (3-5) (2004) 869–891.
- [7] L. Renson, G. Kerschen, Nonlinear Normal Modes of Nonconservative Systems, *Proceedings of IMAC 31th Society of Experimental Mechanics Inc*, February 11-14, Garden Grove, CA, USA (2013), 1–16.
- [8] Y. H. Chong, M. Imregun, Development and Application of a Nonlinear Modal Analysis Technique for MDOF Systems, *Journal of Vibration and Control* 7 (2) (2000) 167–179.
- [9] C. Gibert, Fitting measured frequency response using non-linear modes, *Mechanical Systems and Signal Processing* 17 (1) (2003) 211–218.
- [10] G. Kerschen, J.-c. Golinval, A. F. Vakakis, L. Bergman, The Method of Proper Orthogonal Decomposition for Dynamical Characterization and Order Reduction of Mechanical Systems: An Overview, *Nonlinear Dynamics* 41 (1) (2005) 147–169.

- [11] Y. S. Lee, A. F. Vakakis, D. M. McFarland, L. A. Bergman, A global-local approach to nonlinear system identification: A review, *Structural Control and Health Monitoring* 17 (7) (2010) 742–760.
- [12] A. Y. Leung, Nonlinear modal analysis of frames by the incremental harmonic-balance method, *Dynamics and Stability of Systems* 7 (1) (1992) 43–58.
- [13] P. Ribeiro, M. Petyt, Non-linear free vibration of isotropic plates with internal resonance, *International Journal of Non-Linear Mechanics* 35 (2) (2000) 263–278.
- [14] B. Cochelin, C. Vergez, A high order purely frequency-based harmonic balance formulation for continuation of periodic solutions, *Journal of Sound and Vibration* 324 (1–2) (2009) 243–262.
- [15] D. Laxalde, F. Thouverez, Complex non-linear modal analysis for mechanical systems Application to turbomachinery bladings with friction interfaces, *Journal of Sound and Vibration* 322 (4–5) (2009) 1009–1025.
- [16] M. Krack, L. Panning-von Scheidt, J. Wallaschek, A Method for Nonlinear Modal Analysis and Synthesis: Application to Harmonically Forced and Self-Excited Mechanical Systems, accepted for publication in *Journal of Sound and Vibration*, doi:10.1016/j.jsv.2013.08.009.
- [17] M. Krack, L. Panning-von Scheidt, J. Wallaschek, A. Hartung, C. Siewert, Reduced Order Modeling Based on Complex Nonlinear Modal Analysis and its Application to Bladed Disks With Shroud Contact, Paper GT2013-94560, *Proceedings of ASME Turbo Expo 2013*, June 3–7, San Antonio, TX, USA (2013), 11pp.
- [18] F. Blanc, C. Touzé, J.-F. Mercier, K. Ege, A.-S. Bonnet Ben-Dhia, On the numerical computation of nonlinear normal modes for reduced-order modelling of conservative vibratory systems, *Mechanical Systems and Signal Processing* 36 (2) (2013) 520–539.

- [19] L. I. Manevitch, The Description of Localized Normal Modes in a Chain of Nonlinear Coupled Oscillators Using Complex Variables, *Nonlinear Dynamics* 25 (1-3) (2001) 95–109.
- [20] Y. S. Lee, G. Kerschen, A. F. Vakakis, P. Panagopoulos, L. Bergman, D. M. McFarland, Complicated dynamics of a linear oscillator with a light, essentially nonlinear attachment, *Physica D: Nonlinear Phenomena* 204 (1–2) (2005) 41–69.
- [21] A. F. Vakakis, O. V. Gendelman, G. Kerschen, L. A. Bergman, D. M. McFarland, Y. S. Lee, *Nonlinear targeted energy transfer in mechanical and structural systems*, Springer, 2008.
- [22] A. Vakakis, L. Manevitch, Y. Mikhlin, V. Pilipchuk, A. Zevin, *Normal modes and localization in nonlinear systems*, John Wiley & Sons, 2008.
- [23] T. M. Cameron, J. H. Griffin, An Alternating Frequency/Time Domain Method for Calculating the Steady-State Response of Nonlinear Dynamic Systems, *Journal of Applied Mechanics* 56 (1) (1989) 149–154.
- [24] J. Guillen, C. Pierre, An Efficient, Hybrid, Frequency-Time Domain Method for the Dynamics of Large-Scale Dry-Friction Damped Structural Systems, *Proc. of the IUTAM Symposium*, August 3-7, Munich, Germany (1998), 1–10.
- [25] M. Krack, L. Panning-von Scheidt, J. Wallaschek, A High-Order Harmonic Balance Method for Systems With Distinct States, *Journal of Sound and Vibration* 332 (21) (2013) 5476–5488.
- [26] G. Kerschen, M. Peeters, J. C. Golinval, A. F. Vakakis, Nonlinear normal modes, Part I: A useful framework for the structural dynamicist: Special Issue: Non-linear Structural Dynamics, *Mechanical Systems and Signal Processing* 23 (1) (2009) 170–194.

- [27] G. v. Groll, D. J. Ewins, The harmonic balance method with arc-length continuation in rotor/stator contact problems, *Journal of Sound and Vibration* 241 (2) (2001) 223–233.
- [28] A. Lazarus, O. Thomas, A harmonic-based method for computing the stability of periodic solutions of dynamical systems, *Comptes Rendus Mécanique* 338 (9) (2010) 510–517.
- [29] P. Sundararajan, S. T. Noah, Dynamics of Forced Nonlinear Systems Using Shooting/Arc-Length Continuation Method—Application to Rotor Systems, *Journal of Vibration and Acoustics* 119 (1) (1997) 9–20.
- [30] W. Szemplinska-Stupnicka, The modified single mode method in the investigations of the resonant vibrations of non-linear systems, *Journal of Sound and Vibration* 63 (4) (1979) 475–489.
- [31] A. H. Nayfeh, D. T. Mook, *Nonlinear oscillations*, John Wiley & Sons, New York 1979.
- [32] P. R. Dahl, Solid friction damping of mechanical vibrations, *AIAA Journal* 14 (1976) 1675–1682.
- [33] E. P. Petrov, Analysis of Flutter-Induced Limit Cycle Oscillations in Gas-Turbine Structures With Friction, Gap, and Other Nonlinear Contact Interfaces, *Journal of Turbomachinery* 134 (6) (2012) 061018–061030.